Supplemental Information for "Self-excited motions of volatile drops on swellable sheets"

Aditi Chakrabarti, Gary P. T. Choi, L. Mahadevan

S1 Movie Captions

Movie 1: Spinning of acetone droplets on swellable PDMS film
On a PDMS film ($H = 9$ μm) afloat aqueous glycerol (50% by volume glycerol in water), acetone droplets with initial volumes $V = 3, 5$ μL form bean shapes with $n = 1$ that spin. Larger drops with initial volumes $V = 10, 40$ μL form multilobed shapes with $n = 5$ and 6 respectively. The clips are in real time. Scale bar denotes 1mm, for all movies.

Movie 2: Keratocyte-like motility of acetone drop on thicker PDMS film
On a PDMS film ($H = 28.5$ μm) afloat aqueous glycerol (50% by volume glycerol in water), an acetone drop with initial volume $V = 30$ μL undergoes oscillatory to and fro motion resembling motility of a keratocyte (skin cell), which is also in realtime.

Movie 3: Cellular migration like motility of acetone droplets on PDMS films
On PDMS films (left: $H = 9$ μm and right: $H = 28.5$ μm) afloat aqueous glycerol (50% by volume glycerol in water), acetone droplets with initial volume $V = 40$ μL form multi-lobes towards later times due to swelling gradients that lead to their

migration-like behavior. Both movies are at 2X speed.

Movie 4: Pulsatile motility visualized at high speed
On a PDMS film ($H = 19.5$ μm) afloat aqueous glycerol (50% by volume glycerol in water), an acetone drop with initial volume $V = 30$ μL undergoes pulsatile, stick-slip motion at the boundary. The movie is played at 0.1X realtime speed, i.e., it is slowed down 10 times to visualize the jumps in the motion of the lobes while they spin. Scale bar denotes 1mm.

Movie 5: Acetone drop on PDMS film with cross hatching highlights swollen film around the drop
On a PDMS film ($H = 50$ μm) afloat aqueous glycerol, an acetone drop with initial volume $V = 50$ μL undergoes oscillatory to and fro motion. A copper mesh kept under the petri dish housing the experimental setup, highlights the swollen region of the film around the drop due to the distance between the grids becoming enlarged than that away from the drop. As the drop size shrinks due to evaporation, it transitions back to having a circular contact rim. The film surrounding the drop relaxes back to flat state as the imbibed solvent leaves due to evaporation.

Movies 6 and 7: Infrared imaging of acetone droplets undergoing rotation
Droplets of acetone placed on PDMS films afloat aqueous glycerol (50% by volume glycerol in water) are imaged from top using an infrared camera, which reveal that the length scale of swelling zone (R, in Movie 6) is about twice the radius (a) of the drops. The region with diameter R is cooler than the surrounding region due to evaporative cooling. Multiple droplets in Movie 7 shows that even when they are very close to each other, they do not coalesce.

Movie 8: Droplet undergoing periodic and relaxation oscillations on thin PDMS strip
The movie shows an acetone droplet (with initial volume $V = 20$ μL, dyed with

methylene blue) oscillating on a thin PDMS strip ($H = 100$ μm, width: 5 mm) clamped on two edges with a sag. Along with the movie, the mechanism of how the oscillations arise are described. The droplet eventually comes to a halt when its size decreases below a critical threshold.

Movie 9: Large drops of acetone on thin films form multiple lobes that show uncoordinated travelling waves at their contact line
On a PDMS film ($H = 12$ μm) afloat aqueous glycerol (50% by volume glycerol in water), a large acetone droplet with initial volume $V = 40$ μL form $n \sim 10$ lobes that do not undergo synchronization transition, therefore showing erratic motion. The lobes at different parts of the drop either undergo clockwise or anticlockwise rotation without any coordinated spinning. The clip is in real time.

Movie 10: Actual versus apparent rotation
(Left) An acetone droplet (initial volume, $V = 10$ μL) on PDMS film ($H = 18$ μm, afloat aqueous glycerol) undergoes actual rotation (with lobe $n = 1$) as depicted by the motion of the neutrally buoyant hollow glass microspheres that translocate with the drop. (Right) An acetone droplet (initial volume, $V = 5$ μL) on PDMS film ($H = 10.5$ μm, afloat aqueous glycerol) undergoes apparent rotation as hollow glass microspheres do not move as much as the liquid and the modes seem to undergo a coordinated traveling wave around its edges. Both movies are played at 0.5X speed.

S2 Fabrication of polydimethylsiloxane membranes afloat aqueous glycerol & droplet excitable motion experiments

The experimental setup shown in Fig. 1(a) (main text) comprised of a thin membrane made of polydimethylsiloxane (PDMS, Sylgard 184, Dow Corning) floating atop an aqueous glycerol solution and its thickness ranged in the order of tens of microns.

The preparation of these films followed a procedure reported previously [1] with some modification, which we briefly reiterate below. A solution of 50% (by volume) glycerol (Fisher Chemical) in deionized water was degassed using house vacuum and 20 ml was added to round polystyrene petri dishes (100 mm diameter). PDMS (Sylgard 184) was mixed in 10:1 ratio (base:cross-linking agent) and thoroughly degassed. Different amounts of the PDMS pregel were gently released on the liquid surface of each petri dish and the weight of the added PDMS pregel was weighed carefully. Due to a positive spreading coefficient between PDMS and aqueous glycerol, the polymer spread across the entire surface of the aqueous glycerol. The samples were kept at room temperature for 45 minutes to allow uniform spreading of the PDMS. The samples were then baked in the oven at 75°C for 2h. The thickness ($\sim$ tens of microns) of the cured films was estimated from the weight and density of the added PDMS mixture. This method of estimating the thickness of the films was verified in previous work [1]. All experiments on the fabricated PDMS films were performed within a week after sample preparation under ambient conditions of room temperature around 22°C and relative humidity around 10%. PDMS films were also prepared using the usual spin coating method where duration of spinning and speed were varied to obtain different thicknesses. The dynamics of the drop rotation on freely floating PDMS films were captured at 100 frames per second using a wide-field microscope Axiozoom V16 (Zeiss) and all image analysis were performed using either ImageJ or Matlab. Each new experiment of drop motion was performed on a fresh location on the floating PDMS membranes. Fig. S1 shows the phase space of the acetone droplets shapes, i.e. number of lobes (n) plotted as a function of the initial volume of the droplets for a wide range of thicknesses of the PDMS membrane.

For the 1D experiments, thin strips of spin coated and cured PDMS films were cut using a fine razor blade and mounted between two cover glass slips with a sag in the film and acetone droplets (colored with methylene blue) were used to study the oscillations. Fig. S2 shows a trace of the center of mass of acetone droplet ($V \sim 20$ μL) on a strip (100 μm thick and 5 mm wide) undergoing periodic oscillations in the beginning of the experiment until the trajectory resembles more like relaxation oscillations towards the later part of the experiment. The droplet comes to a halt

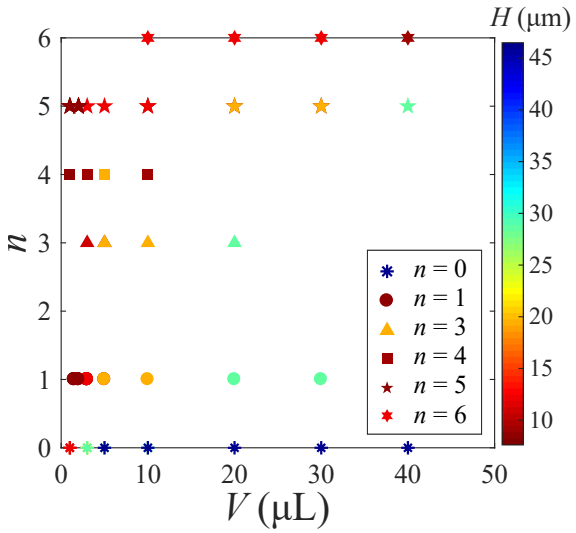

Figure S1: This plot shows the phase space of the number of lobes (n) formed on a given film thickness (H) in an acetone droplet as a function of the initial volume (V), where the color of the symbol represents the thickness of the PDMS film for the respective experiment.

when it is too small to buckle the film (Movie 8).

Varying the height of the underlying aqueous glycerol underneath the film does not affect the phenomenon of drop motion. However, if its height is reduced to less than a millimeter, the drop motion halts implying that the vertical deformations of the film in and out of plane are important for the buckling process of the membrane. In some sense, the liquid underneath provides a homing of the solvent drop and keeps it in a lower potential energy well. To check role played by the liquid underneath the film, experiments were also performed by floating the PDMS films on perfluorodecalin (Sigma Aldrich), which does not wet the PDMS film as well as does not mix with the solvents such as acetone. We observed that acetone drop underwent a few rotations after destabilizing into a multilobed shape, following which it stopped. Our experiments with the PDMS film afloat on a layer of perfluorodecalin suggests that the solvent droplet can undergo spinning for a few cycles as it would if the liquid underneath was aqueous glycerol. However, after a few cycles (over a few seconds),

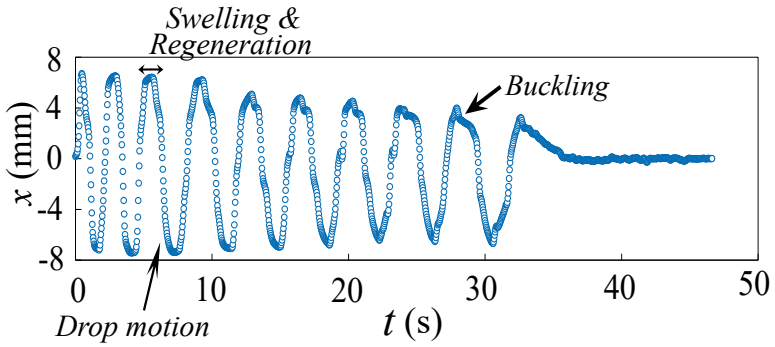

Figure S2: A trace of the x-coordinate of the center of mass of an acetone droplet undergoing periodic oscillations as a function of time, where the different timescales due to swelling of the PDMS film and simultaneous regeneration due to evaporation, and that due to drop motion are indicated. The kinks correspond to the buckling of the film.

the solvent leaving the PDMS film from below collects into a puddle between the film and perfluorodecalin since it is immiscible in perfluorodecalin. For the successful buckling of PDMS film which in turn allows the droplet to form the lobes, the film should be swollen only from one side (in our case, it is from the top, i.e., the droplet side). If there is solvent on both sides of the film (top, due to the drop, and bottom, due to acetone collecting underneath the film), this disallows buckling of PDMS film, which hinders lobe formation and thenceforth any motion. Since aqueous glycerol is miscible with the solvent (acetone in our case), it can absorb it and thereby maintain a solvent free interface between the film and the aqueous glycerol.

S3 Parametric equations for spinning droplets

Note that the shapes of the droplets in general exhibit global rotational symmetry, while the lobes of shapes are locally asymmetric. This observation motivates us to use the following parametric equations to fit each shape:

$$\begin{cases} r(s) = a(1 + b\cos(ns)), \\ \theta(s) = s + \frac{c}{n}\cos(ns + \psi) + \phi. \end{cases} \tag{S1}$$

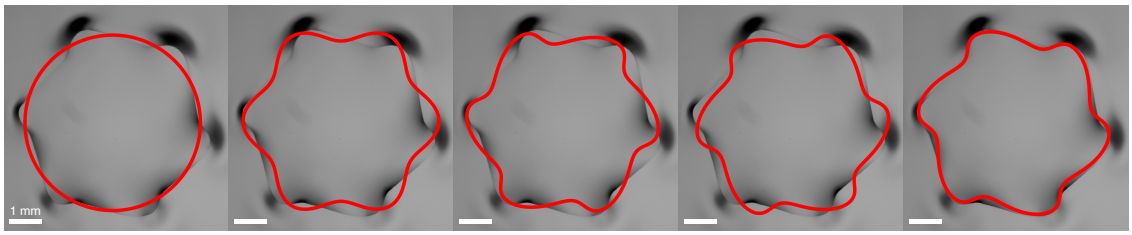

Figure S3: An illustration of the effects of the parameters a, b, c, ψ, ϕ in the parametric equation (S1). Left to right: The fit with a only (with the overall size of the shape captured), the fit with a, b only (with symmetric lobes produced), the fit with a, b, c only (with the symmetry of the lobes broken), the fit with a, b, c, ψ only (with the local phase shift corrected) and the final fit with a, b, c, ψ, ϕ (with the global phase shift corrected).

Here, $(r(s), \theta(s))$ are the polar coordinates of a point on the shape with $s \in (-\pi, \pi]$, $a > 0$ represents the radius of the shape in a global scale, b represents the amplitude of the lobes in a local scale, c accounts for the asymmetry of the lobes, $\psi \in (-\pi, \pi]$ accounts for the local phase shift at the lobes, $\phi \in (-\pi, \pi]$ accounts for the global phase shift, and n is the number of lobes (see Fig. S3 for an illustration of the effects of the parameters).

To obtain the parameters in the above parametric equations for each shape, we first set origin at the center of the shape such that it can be represented as a set of data points in the polar form $\{(r_1, \theta_1), \ldots, (r_k, \theta_k)\}$. Note that n can be obtained by directly counting the number of lobes. We then find the optimal $a, b, c, \psi, \phi, s_1, \ldots, s_k$ that yield the best fit for the following equations for all i:

$$\begin{cases} r_i = a(1 + b\cos(ns_i)), \\ \theta_i = s_i + \frac{c}{n}\cos(ns_i + \psi) + \phi, \end{cases} \tag{S2}$$

where $s_1, \ldots, s_k \in (-\pi, \pi]$. One can further simplify the above problem by combining the two equations and setting

$$s_i = \theta_i - \frac{c}{n}\cos\left[\cos^{-1}\left(\frac{\frac{r_i}{a} - 1}{b}\right) + \psi\right] - \phi, \tag{S3}$$

so that we only need to search for the best fit a, b, c, ψ, ϕ. We remark that if $n = 0$, we have a perfect circle $r = a$ and all other parameters can be omitted.

The symmetry-breaking of the droplet-film system can be parameterized by the ratio of drop size a to the elastocapillary length $\ell = \sqrt{EH^3/T}$, where T is the tension in the film ($T \sim EH\varepsilon_{cap}$, where ε_{cap} is the elastic strain in the film) denoted by the elastocapillary number $a/\ell \sim \sqrt{\varepsilon_{cap}}/\varepsilon_b$, where $\varepsilon_b \sim H/a$ is the buckling strain. The vertical component of surface tension of the droplet ($\gamma_{lv} \sin\theta_c$) can deform the thin film at the contact line due to a strain $\varepsilon_{cap} \sim \gamma_{lv} \sin\theta_c/EH$, where γ_{lv} is the surface tension of the droplet and θ_c is its contact angle with the film. Substituting for the tension gives us the scaling for the elastocapillary length, $\ell \sim \sqrt{EH^3/\gamma_{lv}}$, which has been used to calculate the $a/\ell \sim \sqrt{\varepsilon_{cap}}/\varepsilon_b$ values in Figure 3(b) in the main text.

Table S1 records the best fit parameters for some representative droplets and Fig. S4 shows the best fit parametric curves overlaid on the images of the same droplets.

S4 Péclet numbers of various solvents evaporating from PDMS films

To understand whether other solvents also show the self-generated spinning motion, we carried out experiments with fixed volume (20 μl) of various solvents such as methanol, ethanol, isopropanol, acetone, n-butanol, hexane and chloroform (Fig. S5) on varying film thicknesses. These solvents were picked such that they vary in their ability to swell PDMS [2], evaporation rates and diffusivity through the PDMS network (Table S2). Solvents such as ethanol and methanol, when deposited on the PDMS films, did not show any lobe formation and evaporated with time maintaining their spherical cap shapes. Isopropanol, n-butanol and acetone showed similar lobe formation like acetone for intermediate film thicknesses. Hexane and chloroform swelled PDMS films very rapidly and the film underwent chaotic motion. Therefore, to understand the qualitative differences between the different behaviors of the above mentioned solvents, we systematically measured the evaporative flux J (Table S2)

$H(\mu\text{m})$	$V(\mu\text{L})$	n	$a(\text{mm})$	b	c	ψ	ϕ
9.0	1	0	0.87	0	0	0	0
9.0	3	1	1.27	-0.15	0.85	2.69	0.52
9.0	3	4	1.27	0.05	0.05	-0.45	1.19
9.0	5	1	1.70	0.15	0.95	2.83	-1.05
9.0	5	3	1.70	-0.12	0.65	-0.65	0.28
9.0	5	4	1.69	0.10	-0.14	-1.18	-0.03
9.0	10	4	2.20	-0.15	0.49	-2.72	-0.07
9.0	10	5	2.33	0.08	0.00	1.57	0.13
9.0	20	5	2.77	-0.10	0.52	3.14	-0.15
9.0	30	5	3.47	-0.11	0.40	0.26	0.27
9.0	40	6	3.80	-0.10	0.16	0.21	0.00
12.0	1	0	0.75	0	0	0	0
12.0	3	5	1.27	0.08	0.22	-3.14	0.63
12.0	5	5	1.57	0.08	-0.30	-3.14	1.05
12.0	10	5	2.17	0.10	-0.40	0.2	-0.10
12.0	10	6	2.23	-0.06	-0.40	-3.14	0.02
12.0	20	6	2.67	0.10	0.50	3.14	0.23
12.0	30	6	3.07	-0.10	0.35	3.14	0.20
19.5	3	0	1.24	0	0	0	0
19.5	5	1	2.10	0.55	0.30	-0.50	0.30
19.5	5	3	2.29	0.10	0.25	1.50	0.45
19.5	5	4	2.21	0.10	0.05	0.00	0.66
19.5	10	1	3.00	0.35	-0.85	-0.15	-1.20
19.5	10	3	2.83	-0.15	-0.05	0.07	-0.15
19.5	20	5	4.05	0.10	0.40	0.00	1.45
19.5	30	5	4.62	-0.10	0.45	3.14	0.17
28.5	3	0	1.29	0	0	0	0
28.5	5	0	1.71	0	0	0	0
28.5	10	0	2.09	0	0	0	0
28.5	20	1	2.80	0.50	0.70	-0.31	0.73
28.5	20	3	2.90	0.15	0.50	0.00	0.20
28.5	30	1	3.13	-0.55	0.65	3.14	1.14
28.5	40	5	3.81	0.13	-0.60	-2.66	-0.23
46.5	5	0	1.49	0	0	0	0
46.5	10	0	2.15	0	0	0	0
46.5	20	0	2.70	0	0	0	0
46.5	30	0	3.43	0	0	0	0
46.5	40	0	3.89	0	0	0	0

Table S1: The best fit parameters a, b, c, ψ, ϕ for the parametric equation fitting the outlines of the acetone droplets. H, V, n are the film thickness, drop volume and number of lobes observed respectively.

from solvent-soaked PDMS films (area ~ 1 cm^2) by using a sensitive weighing balance that directly read how the weight of the soaked film decreased as a function of

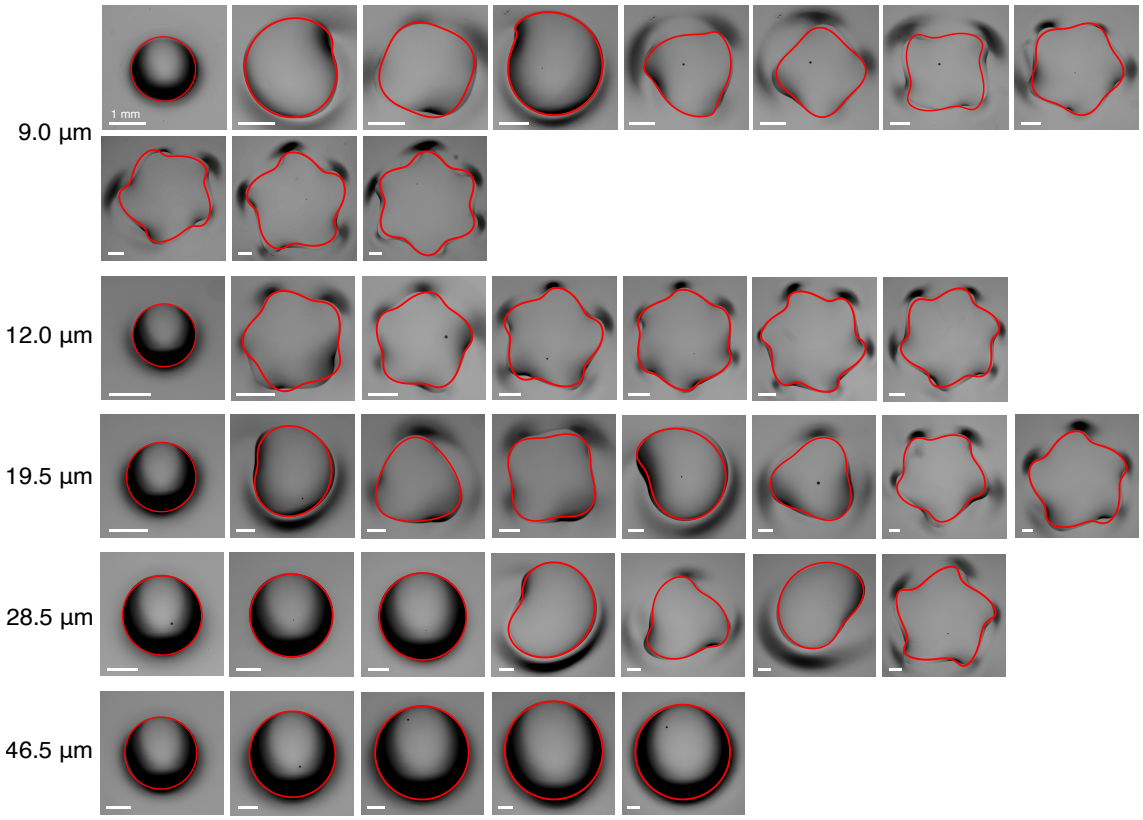

Figure S4: The best fit parametric curves overlaid on the images of the acetone droplets. The scale bar on each image represents 1mm.

time. There could be more sophisticated ways to detect vapor loss from films [3, 4, **?**] but qualitatively both the techniques will yield the same order of magnitude values for the evaporation rates. The Péclet number in each case was then determined as: $Pe \sim \eta Ja^2/kEH$. Here, k is the permeability of the drained porous PDMS network ($\sim (3K_BT/E)^{2/3} = 3.3 \times 10^{-18}$ m^2), E is the Young's modulus of PDMS (2 MPa) and η is the dynamic viscosity of each solvent. Computing the Péclet number for all solvents through the PDMS membranes, we find it to be $\mathcal{O}(10)$ where we see the spontaneous pulsatile motion, while $Pe \lesssim 10$ for all other solvents that do not show any lobe formation and spinning. A direct estimation of a PDMS film (100 μm thick) swollen with acetone drop under the microscope shows that its thickness increases

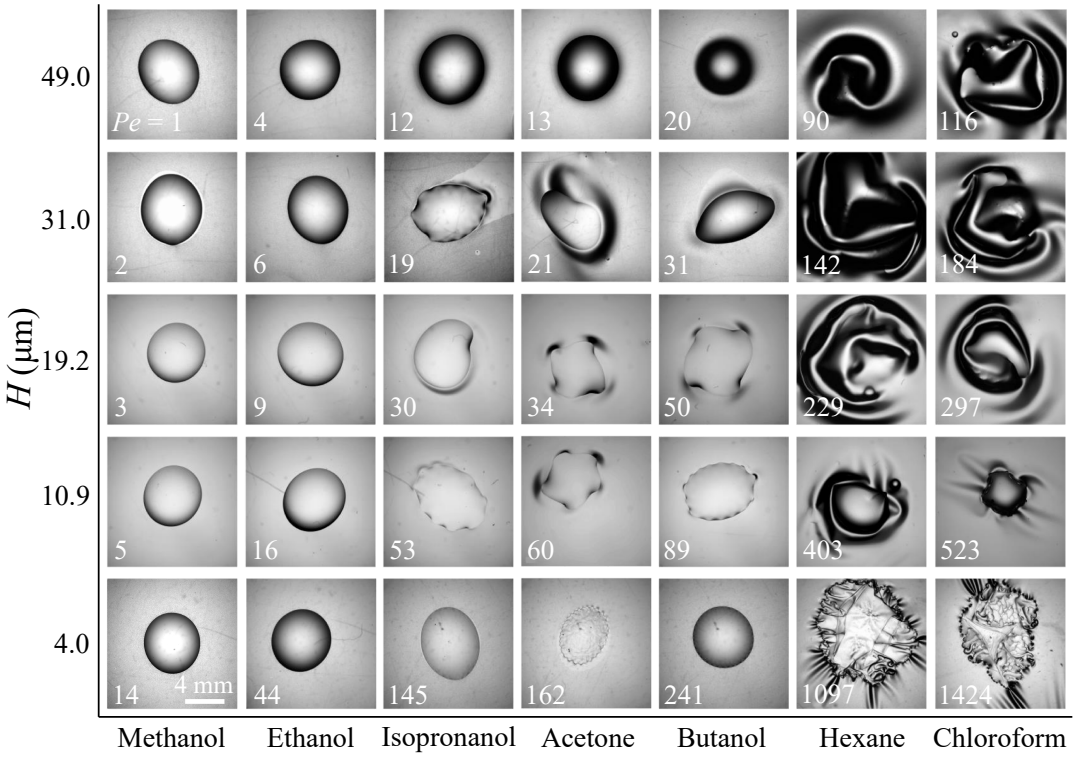

Figure S5: Snapshots of the different shapes assumed by 20 μL droplets of various solvents on different PDMS film thicknesses afloat aqueous glycerol. The respective Péclet numbers are printed in each snapshot corresponding to a specific liquid and a film thickness.

Figure S6: A PDMS film that is mounted vertically on a glass cover slip between two rigid epoxy posts swells to about 20% its original thickness when immersed in acetone (dyed with methylene blue) and reduces to its original thickness when acetone evaporates.

by approximately 20%-25% (Fig. S6).

Solvent	Density, ρ (kg/m^3)	Dynamic viscosity, η (Pa·s)	Evaporative flux measured through PDMS film, J (m/s)	Diffusivity, $D = kE/\eta$ (m^2/s)	Péclet #, $Pe = Ja^2/DH$	Swelling degree, S ([2])	Surface Tension (mN/m)
Acetone	780	3.16E-04	5.42E-07	2.09E-08	20.772	0.295	25
Butanol	810	2.80E-03	9.10E-08	2.36E-09	30.894	0.200	25
Isopropanol	786	2.04E-03	7.51E-08	3.24E-09	18.561	0.162	23
Ethanol	789	1.09E-03	4.30E-08	6.05E-09	5.683	0.063	22
Methanol	792	5.44E-04	2.70E-08	1.21E-08	1.780	-	23
Hexane	655	3.00E-04	3.86E-06	2.20E-08	140.458	-	20
Chloroform	1490	5.36E-04	2.81E-06	1.23E-08	182.264	1.530	27

Table S2: Péclet numbers and other physical properties of solvents studied on the PDMS films, estimated for $H = 20$ μm and $a = 4$ mm. The swelling degrees [2], S, for methanol and hexane are expected to be similar to ethanol and chloroform respectively.

S5 Thermal Marangoni effect in the droplets

In the following, we discuss the role of surface tension gradients in the droplet instability. As we already mentioned in the manuscript, our droplets are composed of one liquid and hence, we do not expect any compositional Marangoni effects to arise. However, thermal effects could lead to surface tension gradients as well. The thermal Marangoni number (Ma $= -\Delta\gamma L/\eta\alpha$) indicates the ratio of the thermal surface tension effects to thermal diffusion. Here, the gradient of surface tension $\Delta\gamma$ is estimated as $(\partial\gamma/\partial T)\Delta T$, where ΔT is the temperature difference across the size of the droplet L, η is the dynamic viscosity and α is the thermal diffusivity of the liquid, values of which are available in data banks [6]. If Ma$\gg$ 1, thermal surface tension gradient should drive flow within the drop and if Ma << 1, thermal diffusion should be the dominant effect. Thermal Marangoni numbers calculated for typical droplet volumes (20 μL) of the various solvents studied in our system are: Methanol, Ma=460; Acetone, Ma =1560; Butanol, Ma=101; Hexane, Ma = 1220 (Table S3). For all the calculations, ΔT was estimated from the IR movies 6 and 7 (SI) during droplet motion. In SI Fig. S5, for film thickness, H=19.2 μm, we see that methanol does not show pattern formation and sits as a hemispherical cap as it evaporates,

Solvent	Surface tension gradient $\partial\gamma/\partial T$ (mN/m.K)	Thermal diffusivity α (m^2/s)	Marangoni # Ma=$-(\partial\gamma/\partial T)\Delta TL/\eta\alpha$
Acetone	-0.13	8.3 E-08	1560
Butanol	-0.08	8 E-08	101
Methanol	-0.08	9.7 E-08	458
Hexane	-0.1	8.5 E-08	1220

Table S3: Marangoni numbers and relevant physical properties for solvents studied on the PDMS films. Values for α and $\partial\gamma/\partial T$ are obtained from Ref. [6]

acetone and butanol show 4 lobes and undergo spinning, hexane shows chaotic wrinkling and no coordinated motion. Since for all the liquids studied here, Ma$\gg$ 1, it suggests that despite having a large thermal Marangoni number, methanol, ethanol and hexane do not show the droplet instability, and are not sufficient conditions to drive the spontaneous motion as is seen in the case of acetone and butanol.

References

[1] Chakrabarti, A. & Chaudhury, M. K. Attraction of Mesoscale Objects on the Surface of a Thin Elastic Film Supported on a Liquid. *Langmuir* **31**, 1911–1920 (2015).

[2] Favre, E. Swelling of crosslinked polydimethylsiloxane networks by pure solvents: influence of temperature. *Eur. Polym. J* **32**, 1183–1188 (1996).

[3] Dehaeck, S. & Rednikov, A.& Colinet, P. Vapor-based interferometric measurement of local evaporation rate and interfacial temperature of evaporating droplets. *Langmuir* **30**, 2002–2008 (2014).

[4] Gatapova, E. Y. & Shonina, A. M.& Safonov, A. I.& Sulyaeva, V. S.& Kabov, O. A. Evaporation dynamics of a sessile droplet on glass surfaces with fluoropolymer coatings: focusing on the final stage of thin droplet evaporation. *Soft Matter* **14**, 1811–1821 (2018).

[5] Sadafi, H.& Dehaeck, S. & Rednikov, A. Vapor-Mediated versus Substrate-Mediated Interactions between Volatile Droplets. *Langmuir* **35**, 7060–7065 (2019).

[6] Dortmund Data Bank http://www.ddbst.com/ddb.html.